

Non-oscillatory gravitational quasinormal modes of Reissner-Nordström-de Sitter spacetime

Z. Stuchlík^{1,*} and A. Zhidenko^{1,2,†}

¹*Research Centre for Theoretical Physics and Astrophysics,
Institute of Physics, Silesian University in Opava,
Bezručovo náměstí 13, CZ-74601 Opava, Czech Republic*

²*Centro de Matemática, Computação e Cognição (CMCC), Universidade Federal do ABC (UFABC),
Rua Abolição, CEP: 09210-180, Santo André, SP, Brazil*

Proper oscillation frequencies of black holes (quasinormal modes) of asymptotically de Sitter black holes were extensively studied, yet the non-oscillatory (purely imaginary) branch of modes of gravitational perturbations of the four-dimensional Reissner-Nordström-de Sitter solution was omitted in the literature. This branch of modes appears as deformations of the modes of empty de Sitter space. Here we find accurate numerical values of this branch of quasinormal modes and show that they are responsible for the exponential asymptotic tails.

PACS numbers: 04.30.Nk, 04.50.+h

I. INTRODUCTION

Quasinormal modes (QNMs) [1–5] represent fundamental oscillatory characteristics of black-hole geometries, emerging naturally as resonant frequencies of perturbations in the spacetime surrounding black holes. These modes are directly observable through gravitational wave signals detected by observatories such as LIGO and Virgo [6–8], providing a powerful tool for probing the properties of black holes and testing general relativity in the strong-field regime. Consequently, QNMs of a wide array of black hole models, including both classical and exotic configurations, have been extensively investigated across an enormous number of papers.

Considerable literature is devoted to quasinormal spectra of black holes in various large scale cosmological environments [9–14]. Particularly, the spectra of quasinormal modes in asymptotically de Sitter spacetimes have attracted significant attention [15–41]. These studies are not only motivated by the growing evidence for a positive cosmological constant from observational cosmology but also by the distinctive features of the quasinormal spectrum due to existence of the de Sitter horizon. The interest in QNMs has been further stimulated by the proposed implications of the Strong Cosmic Censorship limit [42–47].

A peculiar aspect of perturbations in asymptotically de Sitter spacetimes lies in their late-time behavior. Unlike asymptotically flat spacetimes, where perturbations typically decay following a power-law tail [48], in de Sitter spacetimes *exponential tails* prevail at late times. This behavior was first demonstrated for scalar field perturbations in [49] and later for gravitational perturbations and fields of nonzero spin in [50]. However, accurately identifying the asymptotic tail behavior from numerical

simulations remains a challenging task due to the intricate dependence of the decay law on various physical parameters [51]. The nature of these exponential tails was revealed in [52, 53], where it was shown that the exponential tails of the Schwarzschild-de Sitter black hole represent a distinct phase of the quasinormal ringing, governed by purely imaginary quasinormal modes. Unlike the algebraically special mode, these purely imaginary modes satisfy the ingoing boundary condition at the event horizon and thus indeed belong to the quasinormal spectrum. Notably, as the black hole mass approaches zero, these modes go over to the modes of the empty de Sitter spacetime [42, 54–56]. In the limit of a vanishing cosmological constant, the purely imaginary quasinormal frequencies asymptotically approach zero, indicating that these modes dominate the spectrum with the lowest damping rate when the cosmological constant is small, suggested by observational cosmology. It is worth mentioning that this branch of de Sitter modes breaks down the correspondence between null geodesics and eikonal quasinormal modes [57].

For the Reissner-Nordström-de Sitter spacetime, purely imaginary quasinormal modes were previously identified for a test scalar field [42, 56]. However, to the best of our knowledge, a comprehensive analysis of such modes within the gravitational sector, which also includes the electromagnetic perturbations, has not yet been conducted.

In this work, we address this gap by calculating the purely imaginary quasinormal modes of gravitational perturbations of the Reissner-Nordström-de Sitter black hole. We employ the Leaver method to determine these modes in the frequency domain. Furthermore, by integrating the wave equation in the time domain, we demonstrate that the observed exponential tails are, in fact, a manifestation of these purely imaginary quasinormal modes.

Our paper is organized as follows: In Sec. II we give the basic formulas on the black hole metric and the form of

* zdenek.stuchlik@physics.slu.cz

† olexandr.zhidenko@ufabc.edu.br

the wave equation describing coupled gravitational and electromagnetic perturbations. Sec. III is devoted to the brief description of the numerical methods we use: Leaver method and time-domain integration. Sec. IV discusses the quasinormal spectrum of the Reissner-Nordström-de Sitter spacetime: Particularly, in Sec. IV B we discuss the features of the de Sitter branch of the quasinormal spectrum, associated with perturbations of de Sitter universe and in Sec. IV C its interplay with the branch of complex modes, associated with the black hole. Finally, in the Conclusions we summarize the obtained results.

II. BASIC FORMULAS

Here we will use the convenient formalism for 4-dimensional Reissner-Nordström-de Sitter black holes and designations of [58–60], taking then $D = n + 2 = 4$. The metric has the following form:

$$ds^2 = f(r)dt^2 - \frac{dr^2}{f(r)} - r^2(d\theta^2 + \sin^2\theta d\phi^2). \quad (1)$$

where

$$\begin{aligned} f(r) &= 1 - X + Z - Y, \\ X &= \frac{2M}{r}, \quad Y = \frac{\Lambda r^2}{3}, \quad Z = \frac{Q^2}{r^2}. \end{aligned} \quad (2)$$

The perturbation equations can be reduced to the wave-like form [60]:

$$\left(\frac{\partial^2}{\partial t^2} - \frac{\partial^2}{\partial r_*^2} \right) \Psi(t, r) = -V(r)\Psi(t, r), \quad (3)$$

where *the tortoise coordinate* r_* is defined as

$$dr_* = \frac{dr}{f(r)}. \quad (4)$$

The effective potentials for the decoupled vector (axial) gravitational and electromagnetic perturbations are

$$V_{V\pm}(r) = \frac{f(r)}{r^2} \left(\lambda + 2 + \frac{8Z - 3X \pm \sqrt{9X^2 + 16Z\lambda}}{2} \right), \quad (5)$$

where

$$\lambda \equiv (\ell + 2)(\ell - 1) > 0,$$

and $\ell = 2, 3, 4, \dots$ is the multipole number.

We note that, since $X^2/Z \equiv 4M^2/Q^2$ is a constant, the effective potential (5) is a rational function of the radial coordinate r .

The effective potentials for the decoupled perturbations of scalar (polar) type are

$$V_{S\pm}(r) = f(r) \frac{\tilde{U}_{\pm}(r)}{r^2 H_{\pm}(r)^2}, \quad (6)$$

where

$$\begin{aligned} H_+(r) &= 1 - 3X\delta, \\ H_-(r) &= \lambda + 3X(1 + \delta\lambda), \\ \tilde{U}_+(r) &= -162X^4\delta^3(1 + \delta\lambda) + 36X^3\delta^2(3\delta\lambda + 4) \\ &\quad - 36X^2\delta(2Y\delta + 1) - 12X\delta\lambda + 4\lambda + 8, \\ \tilde{U}_-(r) &= -162X^4\delta(1 + \delta\lambda)^3 - 36X^3(1 + \delta\lambda)^2(3\delta\lambda - 1) \\ &\quad - 36X^2(1 + \delta\lambda)(2Y(1 + \delta\lambda) - \lambda) \\ &\quad + 12X\lambda^2(1 + \delta\lambda) + 4\lambda^3 + 8\lambda^2, \end{aligned}$$

and the constant δ is defined as follows:

$$\delta \equiv \frac{1}{2\lambda} \left(\sqrt{1 + \frac{4\lambda Q^2}{9M^2}} - 1 \right) = \frac{1}{2\lambda} \left(\sqrt{1 + \frac{16Z\lambda}{9X^2}} - 1 \right).$$

In the limit of zero charge $Q = 0$ ($Z = 0$, $\delta = 0$), the potentials V_{V+} and V_{S+} reduce to the potential of a test Maxwell field, and the potentials V_{V-} and V_{S-} correspond to the axial and polar gravitational perturbations, respectively, in the Schwarzschild-de Sitter background.

For $\ell = 1$, only the perturbations of the Maxwell field are dynamical (see Sec. 4.2.2 of [60] for details). These perturbations are governed by the effective potential

$$V_{\ell=1}(r) = \frac{2f(r)}{r^2}. \quad (7)$$

In four-dimensional spacetime, axial and polar perturbations are governed by equations related through a Darboux transformation, meaning that the solution for one can be derived from the other. As a result, the quasinormal spectra of V_{V+} and V_{S+} , as well as those of V_{V-} and V_{S-} , are identical [51]. From this point forward, we will refer to these modes as “+” and “−”, respectively.

To simplify the analysis, we introduce the following geometric quantities: the radius of the event horizon r_h , the cosmological horizon r_c , and the inner horizon r_i [61]. We can easily express the black hole mass M , the cosmological constant Λ , and the electric charge Q in terms of

$$0 \leq r_i \leq r_h < r_c \leq \infty. \quad (8)$$

First, using that the metric function vanishes at the event horizon, we find that

$$2M = r_h + \frac{Q^2}{r_h} - \frac{\Lambda r_h^3}{3}. \quad (9)$$

Using the similar condition for the cosmological horizon we express the Λ -term,

$$\frac{\Lambda}{3} = \frac{r_c r_h - Q^2}{r_c r_h (r_c^2 + r_c r_h + r_h^2)}. \quad (10)$$

Finally, we express the value of Q in terms of the inner horizon,

$$Q^2 = \frac{r_c r_h r_i (r_c + r_h + r_i)}{r_c^2 + r_h^2 + r_i^2 + r_c r_h + r_c r_i + r_h r_i}. \quad (11)$$

The uncharged black hole corresponds to $r_i = 0$, so that $Q = 0$. When $r_i = r_h$, we have the extremely charged black hole, $f'(r_h) = 0$. The limit $r_c \rightarrow \infty$ yields the asymptotically flat Reissner-Nordström black-hole solution with $\Lambda = 0$ and $Q^2 = r_h r_i$.

III. NUMERICAL METHODS

In this section, we summarize the methods used to calculate quasinormal frequencies. We employ the Leaver method [62] in the frequency domain and verify the obtained results in the time domain using the Gundlach-Price-Pullin integration scheme [63].

A. Leaver method

In order to switch to the frequency domain, we substitute

$$\Psi(t, r) = e^{-i\omega t} \Psi(r) \quad (12)$$

into the Eq. 3 and obtain for the radial function

$$\frac{d^2 \Psi}{dr_*^2} + (\omega^2 - V(r)) \Psi(r) = 0. \quad (13)$$

Now quasinormal frequencies can be defined as wave equation's eigenvalues ω_n , where n is the overtones number, which correspond specific boundary conditions: purely outgoing waves at the cosmological horizon $r = r_c$ ($r_* \rightarrow +\infty$) and purely ingoing waves at the black hole event horizon $r = r_h$ ($r_* \rightarrow -\infty$).

$$\begin{aligned} \Psi(t, r) &\propto e^{-i\omega(t+r_*)}, \quad r_* \rightarrow -\infty, \\ \Psi(t, r) &\propto e^{-i\omega(t-r_*)}, \quad r_* \rightarrow +\infty, \end{aligned} \quad (14)$$

yielding the following conditions for $\Psi(r)$ at the regular singular points of Eq. (13)

$$\begin{aligned} \Psi(r) &\propto (r - r_h)^{-i\omega/f'(r_h)}, \quad r \rightarrow r_h + 0, \\ \Psi(r) &\propto (r_c - r)^{+i\omega/f'(r_c)}, \quad r \rightarrow r_c - 0. \end{aligned} \quad (15)$$

We study the solution in the interval $r_h < r < r_c$. Therefore, we introduce the new function, $y(r)$, such that

$$\Psi(r) = \left(\frac{r_c - r}{r - r_i} \right)^{i\omega/f'(r_c)} \left(\frac{r - r_h}{r - r_i} \right)^{-i\omega/f'(r_h)} y(r). \quad (16)$$

Here $\Psi(r)$ satisfies the quasinormal boundary conditions (15) iff $y(r)$ is regular at $r = r_h$ and $r = r_c$. We express $y(r)$ in terms of the Frobenius series expansion:

$$y(r) = \sum_{k=0}^{\infty} a_k \left(\frac{r - r_h}{r - r_i} \cdot \frac{r_c - r_i}{r_c - r_h} \right)^k. \quad (17)$$

By accounting for the singular point $r = r_i$ of the Eq. (13), we ensure the convergence of the series (17) for $r_h \leq r < r_c$. The coefficients a_i satisfy a seven-term recurrence relation for vector-type perturbations (5) and a nine-term recurrence relation for scalar-type perturbations (6). These recurrence relations can be numerically reduced to a three-term relation via Gaussian elimination (for details, see [4]). The final step involves solving an

infinite continued fraction equation for ω , which ensures the convergence of the series (17) at $r = r_c$.

In order to improve convergence of the infinite continued fraction for the purely imaginary modes we use the Nollert method [64, 65]. The continued-fraction approach has been discussed and used for finding precise values of quasinormal frequencies in numerous works (see [66–71] for recent examples) and, therefore, we will not review it here in more detail.

B. Time-domain integration

In order to analyze the perturbation evolution at all times and check the values of the quasinormal modes obtained in frequency domain, we use the time-domain integration method. This approach involves solving the master equation (3) in terms of the light-cone coordinates, defined as $u \equiv t - r_*$ and $v \equiv t + r_*$.

For numerical integration, we utilize the discretization scheme, proposed in [63],

$$\begin{aligned} \Psi(N) &= \Psi(W) + \Psi(E) - \Psi(S) \\ &\quad - \Delta^2 V(S) \frac{\Psi(W) + \Psi(E)}{4} + \mathcal{O}(\Delta^4). \end{aligned} \quad (18)$$

In the above relation, the following notations for the points were used: $N \equiv (u + \Delta, v + \Delta)$, $W \equiv (u + \Delta, v)$, $E \equiv (u, v + \Delta)$, and $S \equiv (u, v)$. Then, with the Gaussian initial data on the surfaces, $u = u_0$ and $v = v_0$, we calculate the values of the functions in the rhombus $u_0 < u < u_1$ and $v_0 < v < v_1$. The dominant modes can be extracted from the time-domain profiles with the help of the Prony method, which is based on the fitting of the time-domain profile by a sum of exponents (see, e.g., [4]).

The time-domain integration is an effective method for finding the fundamental mode of asymptotically flat black holes (see [72–84] for recent examples) and a few first overtones for asymptotically de Sitter spacetimes [36, 37], as the comparison with other, more accurate methods, shows.

IV. QUASINORMAL MODES OF THE REISSNER-NORDSTRÖM-DE SITTER SPACETIME

A. Complex modes of the charged black holes

The quasinormal modes of the Reissner–Nordström black hole are modified by the presence of a positive cosmological constant. These modes are generally complex, and in the asymptotically flat limit $\Lambda \rightarrow 0$ (or equivalently $r_c \rightarrow \infty$), they reduce to the corresponding modes of the Reissner–Nordström solution in asymptotically flat spacetime.

In the opposite limit of large black holes, $r_h \rightarrow r_c$, both the real and imaginary parts of the quasinormal

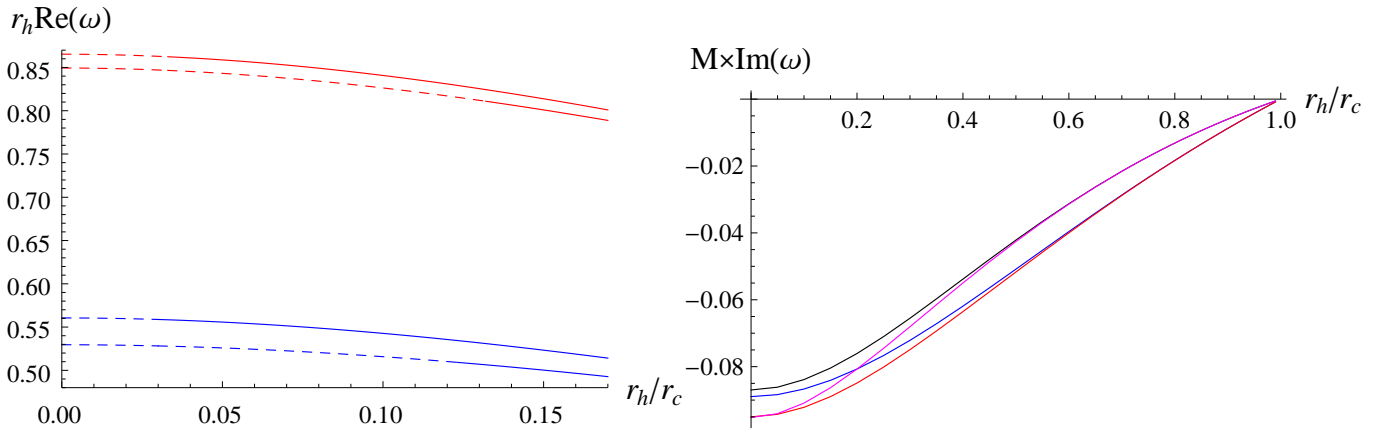


FIG. 1. Dominant $\ell = 2$ mode of the black-hole branch (in units of black-hole mass) for “-” (blue) and “+” (red) perturbations of the uncharged black hole ($r_i = 0$), compared with “-” (black) and “+” (magenta) modes of the charged black hole ($r_i = r_h/2$).

frequencies tend to zero [15], and the frequencies can be expressed as:

$$\omega = \frac{f'(r_h)}{2} \left(A - \left(n + \frac{1}{2} \right) i \right) + \mathcal{O}(r_c - r_h)^2, \quad (19)$$

where n is the overtone number, A is a constant, which depends on the type of perturbations, multipole number ℓ , and the ratio r_i/r_h . For the uncharged black holes ($r_i = 0$) the value of A matches the corresponding quantity for test fields in the Schwarzschild–de Sitter background [22], and is given by:

$$A = \sqrt{(\ell + s)(\ell + 1 - s) - \frac{1}{4}}, \quad (20)$$

where $s = 1$ for the electromagnetic perturbations (“+” modes) and $s = 2$ for the gravitational perturbations (“-” modes).

When the electric charge is nonzero ($r_i > 0$), the qualitative behavior of the quasinormal modes in units of the black-hole mass remains similar to the charged asymptotically flat case [85]. The damping rate changes only slightly with increasing charge, typically decreasing for sufficiently large charge. Meanwhile, the real part of the frequency increases with charge for “+” modes and also for “-” modes when the black hole is relatively small. However, for sufficiently large black holes, specifically when $r_h \gtrsim r_c/2$, the behavior changes: the “-” modes of charged black holes may exhibit a smaller real part of the frequency compared to their uncharged counterparts. This nonmonotonic dependence on the charge is illustrated in Fig. 1, showing the interplay between the cosmological constant and electric charge in shaping the dominant mode.

B. Purely imaginary quasinormal modes

As shown for scalar field perturbations in [42] and for gravitational perturbations in [52], in addition to

the complex branch of modes associated with the black hole, there exists another branch of quasinormal modes that are purely imaginary, meaning they consist of non-oscillatory, exponentially decaying modes. When $r_h \rightarrow 0$, the purely imaginary quasinormal frequencies go over into the modes of the empty de Sitter spacetime [52] $\omega_n^{(dS)}$, which have the following form [54, 55]:

$$\omega_n^{(dS)} r_c = -i(\ell + n + 1 - \delta_{s0} \delta_{n0}), \quad (21)$$

where $n = 0, 1, 2, \dots$ is the overtone number and $\ell = s, s + 1, \dots$ is the multiple number.

These purely imaginary modes of black holes are particularly interesting because they violate the well-known correspondence between eikonal quasinormal modes and null geodesics. According to this correspondence, valid in the limit $\ell \rightarrow \infty$, the real and imaginary parts of the quasinormal frequencies are related to the angular frequency and the Lyapunov exponent of the unstable null geodesics, respectively [86]. This relation holds due to the dominance of the centrifugal term $\propto f(r)\ell^2/r^2$ in the effective potential. Consequently, when the centrifugal term takes an unusual form – as it does in various higher-curvature gravity theories – the correspondence no longer holds [87–89]. The correspondence between null geodesics and the eikonal behavior of quasinormal modes also breaks down for electromagnetic perturbations in nonlinear electrodynamics, where light rays do not follow null geodesics [90]. In our case, although the theory involves standard Maxwell electrodynamics and the centrifugal term retains its usual form, the correspondence still breaks down because the de Sitter branch of modes cannot be captured by the WKB approximation, which is essential for establishing this correspondence [57]. The black-hole branch alone still obeys the correspondence. In addition, the de Sitter branch determines the strong cosmic censorship bound for quasinormal modes when the radius of the event horizon is much smaller than the de Sitter radius [91].

If the radius of the black hole is much smaller than

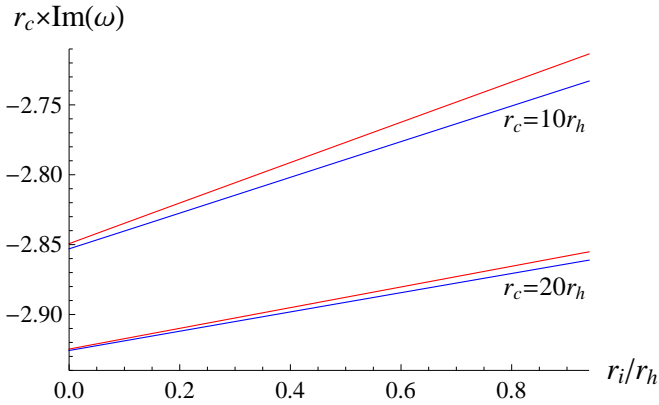


FIG. 2. The lowest purely imaginary quasinormal modes for $\ell = 2$ “-” (blue, lower) and “+” (red, upper) perturbations: $r_c = 10r_h$ (top) and $r_c = 20r_h$ (bottom).

the radius of the cosmological horizon, the quasinormal modes of test fields obey the following *universal law* [91], which is valid not only for the Schwarzschild-de Sitter black hole, but also for any spherically symmetric black hole independently on an underlying metric gravitational theory:

$$\omega_n = \omega_n^{(dS)} \left(1 - \frac{M}{r_c} + \mathcal{O} \left(\frac{M}{r_c} \right)^2 \right). \quad (22)$$

For the coupled electromagnetic and gravitational perturbations the dependence of the purely imaginary branch of modes is remarkably close to the linear function of r_i (see Fig. 2). By fitting the numerical data for $r_h \ll r_c$ we obtain the following approximate formula

$$\omega_n \propto 1 - \frac{r_i}{2r_c}, \quad (23)$$

which confirms that the universal law (22) holds for the gravitational and electromagnetic perturbations of the charged black holes,

$$\frac{\omega_n}{\omega_n^{(dS)}} = 1 - \frac{M}{r_c} + \mathcal{O} \left(\frac{M}{r_c} \right)^2 = 1 - \frac{r_h + r_i}{2r_c} + \mathcal{O} \left(\frac{r_h}{r_c} \right)^2.$$

Surprisingly, the above approximation remains accurate for describing the de Sitter branch of modes even in the presence of a large black hole. As the black-hole mass increases, the decay rate of the purely imaginary mode decreases. However, as illustrated in Fig. 3, it does not vanish in the near-extremal limit, since the black-hole mass satisfies $M < r_h \rightarrow r_c$ and never exactly reaches the cosmological horizon.

C. Interplay between two branches of the quasinormal modes

We are now in a position to present a complete picture of the quasinormal spectrum in Reissner–Nordström–de Sitter spacetime. It consists of two distinct branches:

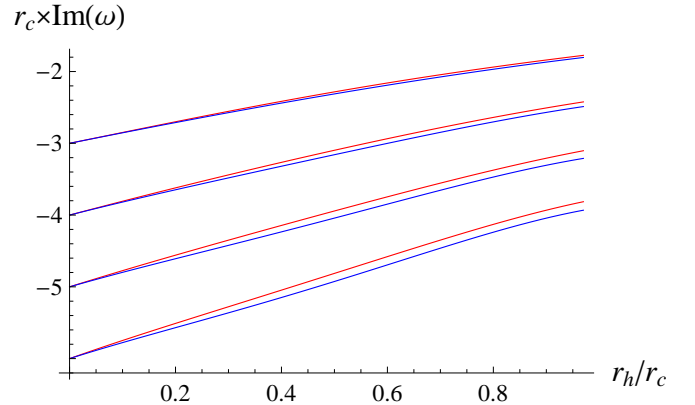


FIG. 3. The lowest purely imaginary quasinormal modes for $\ell = 2$ “-” (blue, lower) and “+” (red, upper) perturbations of the uncharged black hole ($r_i = 0$).

1. *The de Sitter branch*, consisting of purely imaginary modes, which are the least damped when the black hole is small ($r_c \gg r_h$), as the frequencies scale roughly with r_c^{-1} .
2. *The black-hole branch*, consisting of complex modes that approach the Reissner–Nordström spectrum in the asymptotically flat spacetime limit. These modes become the least damped for large black holes, and in the near-extreme limit ($r_h \rightarrow r_c$), their frequencies scale with $r_c - r_h$.

This leads to a peculiar and non-monotonic behavior of the least damped mode as a function of the black-hole radius r_h . For small black holes, the purely imaginary modes of the de Sitter branch have the slowest decay rate. As r_h increases, the damping rate of this mode increases, and eventually a mode of the black-hole branch becomes the least damped. Upon further increase of r_h , the next mode of the black-hole branch (the first overtone) overtakes the purely imaginary mode. As the black hole approaches its extremal size ($r_h \rightarrow r_c$), more and more of the dominant overtones transition from purely imaginary to complex, while the purely imaginary modes are pushed to higher overtone numbers.

Fig. 4 illustrates this transition for charged black holes of varying sizes. For sufficiently small black holes, the two least-damped modes are purely imaginary. At a certain value of r_h , the least-damped $\ell = 2$ “-” mode becomes one from the black-hole branch, followed by a similar transition for the $\ell = 2$ “+” mode. After that, the least-damped purely imaginary mode becomes the first overtone. At larger r_h , the second black-hole mode becomes the first overtone – first for “-” perturbations, and later for “+”. The higher the ratio r_h/r_c , the more overtones transition to modes from the black-hole branch.

It is important to note that, although the purely imaginary modes are the least damped in Reissner–Nordström–de Sitter spacetime when $r_h \ll r_c$, they are typically not observed in the gravitational-wave sig-

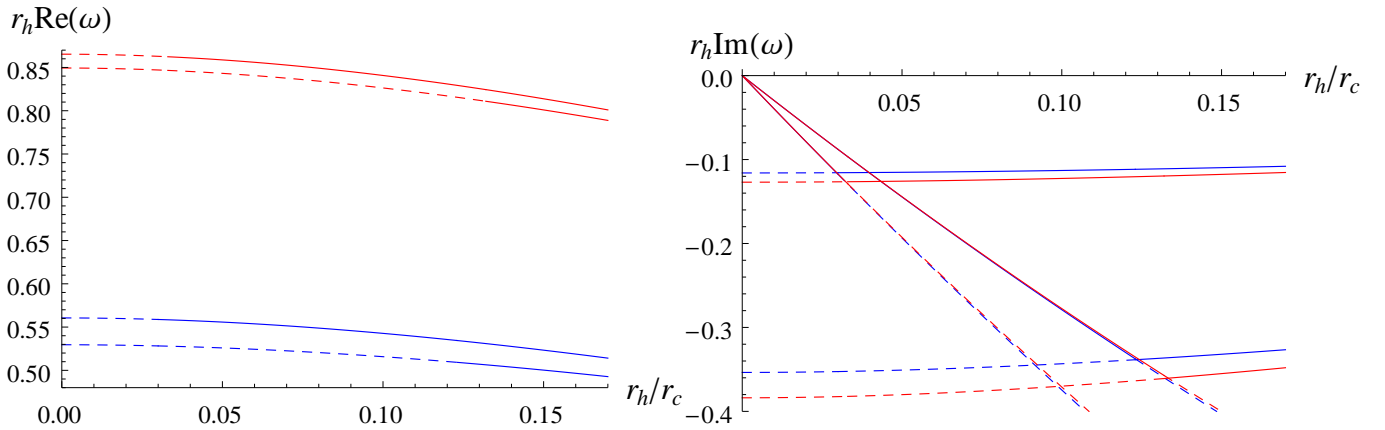


FIG. 4. Two least-damped $\ell = 2$ modes of a charged black hole with $r_i = r_h/2$, shown for “-” (blue) and “+” (red) perturbations. Solid lines indicate the least-damped modes, while dashed lines represent the corresponding modes in the parametric region, when they are not the least damped. For small black holes, the least damped modes are purely imaginary.

nal emitted by a perturbed black hole. These modes appear only at very late times as the so-called exponential asymptotic tails, when the gravitational-wave signal has already decayed significantly. The reason is that the initial perturbation tends to excite the modes associated with the black hole much more strongly than the modes associated with the de Sitter Universe. Therefore, one must carefully distinguish between the full quasinormal spectrum of a spacetime and the subset of modes that are actually observable in a gravitational-wave signal.

V. CONCLUSIONS

The Reissner-Nordström-de Sitter metric describes a classical black-hole solution to the Einstein-Maxwell equations with a cosmological constant. As a result, perturbations and quasinormal modes of both test fields and gravitational perturbations have been extensively studied in the literature [92–98]. However, the spectrum of gravitational perturbations has not been fully explored to date. Of the two branches of modes – the black-hole branch and the de Sitter branch – only the former has been analyzed in detail [51]. In this work, we address this gap by investigating the previously unexplored de

Sitter branch, thereby providing a more complete picture of the quasinormal mode spectrum of this classical black-hole solution. We conducted a comprehensive analysis of the full quasinormal spectrum of the coupled gravitational and electromagnetic perturbations of the Reissner-Nordström-de Sitter black hole. Our study reveals that purely imaginary modes of the de Sitter branch emerge within the gravitational perturbation spectrum of charged black holes and satisfy the universal analytic formula in the regime of small black holes, which was previously obtained only for test fields. This analytic expression provides a good approximation for the modes of the de Sitter branch even as the black-hole size is comparable with the de Sitter radius.

Although the quasinormal modes of the de Sitter branch are the least damped for small black-hole sizes, these modes are not typically observed in gravitational-wave signals. This is because the modes from the black-hole branch tend to be the most strongly excited by the perturbations of black holes. As a result, the modes of the de Sitter branch primarily manifest only as late-time exponential tails, appearing after the main signal has significantly decayed. Consequently, their observational signatures in gravitational-wave data are generally suppressed and difficult to detect.

-
- [1] K. D. Kokkotas and B. G. Schmidt, *Living Rev. Rel.* **2**, 2 (1999), arXiv:gr-qc/9909058.
- [2] E. Berti, V. Cardoso, and A. O. Starinets, *Class. Quant. Grav.* **26**, 163001 (2009), arXiv:0905.2975 [gr-qc].
- [3] H.-P. Nollert, *Class. Quant. Grav.* **16**, R159 (1999).
- [4] R. A. Konoplya and A. Zhidenko, *Rev. Mod. Phys.* **83**, 793 (2011), arXiv:1102.4014 [gr-qc].
- [5] S. V. Bolokhov and M. Skvortsova, (2025), arXiv:2504.05014 [gr-qc].
- [6] B. P. Abbott *et al.* (LIGO Scientific, Virgo), *Phys. Rev. Lett.* **116**, 061102 (2016), arXiv:1602.03837 [gr-qc].
- [7] B. P. Abbott *et al.* (LIGO Scientific, Virgo), *Phys. Rev. Lett.* **119**, 161101 (2017), arXiv:1710.05832 [gr-qc].
- [8] R. Abbott *et al.* (LIGO Scientific, Virgo), *Astrophys. J. Lett.* **896**, L44 (2020), arXiv:2006.12611 [astro-ph.HE].
- [9] R. A. Konoplya, *Phys. Lett. B* **823**, 136734 (2021), arXiv:2109.01640 [gr-qc].
- [10] R. A. Konoplya and E. Abdalla, *Phys. Rev. D* **71**, 084015 (2005), arXiv:hep-th/0503029.
- [11] K. Jusufi, *Phys. Rev. D* **101**, 084055 (2020),

- arXiv:1912.13320 [gr-qc].
- [12] C. Zhang, T. Zhu, and A. Wang, *Phys. Rev. D* **104**, 124082 (2021), arXiv:2111.04966 [gr-qc].
- [13] B. Hamil, A. Al-Badawi, and B. C. Lütfüoğlu, (2025), arXiv:2505.18611 [gr-qc].
- [14] B. C. Lütfüoğlu, *Eur. Phys. J. C* **85**, 486 (2025), arXiv:2503.16087 [gr-qc].
- [15] A. Zhidenko, *Class. Quant. Grav.* **21**, 273 (2004), arXiv:gr-qc/0307012.
- [16] S. Yoshida and T. Futamase, *Phys. Rev. D* **69**, 064025 (2004), arXiv:gr-qc/0308077.
- [17] R. A. Konoplya and A. Zhidenko, *JHEP* **06**, 037 (2004), arXiv:hep-th/0402080.
- [18] V. Cardoso and J. P. S. Lemos, *Phys. Rev. D* **67**, 084020 (2003), arXiv:gr-qc/0301078.
- [19] O. J. Tattersall, *Phys. Rev. D* **98**, 104013 (2018), arXiv:1808.10758 [gr-qc].
- [20] A. Aragón, P. A. González, E. Papantonopoulos, and Y. Vásquez, *JHEP* **08**, 120 (2020), arXiv:2004.09386 [gr-qc].
- [21] P. Hintz and Y. Xie, *J. Math. Phys.* **63**, 011509 (2022), arXiv:2105.02347 [gr-qc].
- [22] M. S. Churilova, R. A. Konoplya, and A. Zhidenko, *Phys. Rev. D* **105**, 084003 (2022), arXiv:2108.04858 [gr-qc].
- [23] A. Roussev, *Gen. Rel. Grav.* **54**, 80 (2022).
- [24] R. A. Konoplya and A. Zhidenko, *Phys. Rev. D* **76**, 084018 (2007), [Erratum: *Phys. Rev. D* **90**, 029901 (2014)], arXiv:0707.1890 [hep-th].
- [25] S. Dyatlov, *Annales Henri Poincaré* **13**, 1101 (2012), arXiv:1101.1260 [math.AP].
- [26] R. A. Konoplya, *Phys. Rev. D* **68**, 124017 (2003), arXiv:hep-th/0309030.
- [27] C. Molina, *Phys. Rev. D* **68**, 064007 (2003), arXiv:gr-qc/0304053.
- [28] S. Fernando, *Int. J. Mod. Phys. D* **24**, 1550104 (2015), arXiv:1508.03581 [gr-qc].
- [29] J. Natario and R. Schiappa, *Adv. Theor. Math. Phys.* **8**, 1001 (2004), arXiv:hep-th/0411267.
- [30] R. A. Konoplya and A. Zhidenko, *Phys. Rev. Lett.* **103**, 161101 (2009), arXiv:0809.2822 [hep-th].
- [31] R. A. Konoplya and A. Zhidenko, *Phys. Rev. D* **95**, 104005 (2017), arXiv:1701.01652 [hep-th].
- [32] B. Toshmatov and Z. Stuchlík, *Eur. Phys. J. Plus* **132**, 324 (2017), arXiv:1707.07419 [gr-qc].
- [33] M. A. Cuyubamba, R. A. Konoplya, and A. Zhidenko, *Phys. Rev. D* **93**, 104053 (2016), arXiv:1604.03604 [gr-qc].
- [34] R. A. Konoplya and A. Zhidenko, *Phys. Rev. D* **89**, 024011 (2014), arXiv:1309.7667 [hep-th].
- [35] R. A. Konoplya, A. Khrabustovskyi, J. Kříž, and A. Zhidenko, (2025), arXiv:2501.16134 [gr-qc].
- [36] A. Dubinsky, *Mod. Phys. Lett. A* **39**, 2450108 (2024), arXiv:2404.18004 [gr-qc].
- [37] A. Dubinsky and A. Zinhailo, *Eur. Phys. J. C* **84**, 847 (2024), arXiv:2404.01834 [gr-qc].
- [38] R. A. Konoplya and A. Zhidenko, *Class. Quant. Grav.* **40**, 245005 (2023), arXiv:2309.02560 [gr-qc].
- [39] R. A. Konoplya, *Phys. Rev. D* **103**, 044033 (2021), arXiv:2012.13020 [gr-qc].
- [40] P. Kanti and R. A. Konoplya, *Phys. Rev. D* **73**, 044002 (2006), arXiv:hep-th/0512257.
- [41] Z. Malik, *Z. Naturforsch. A* **79**, 1063 (2024).
- [42] V. Cardoso, J. a. L. Costa, K. Destounis, P. Hintz, and A. Jansen, *Phys. Rev. Lett.* **120**, 031103 (2018), arXiv:1711.10502 [gr-qc].
- [43] O. J. C. Dias, F. C. Eperon, H. S. Reall, and J. E. Santos, *Phys. Rev. D* **97**, 104060 (2018), arXiv:1801.09694 [gr-qc].
- [44] O. J. C. Dias, H. S. Reall, and J. E. Santos, *Class. Quant. Grav.* **36**, 045005 (2019), arXiv:1808.04832 [gr-qc].
- [45] Y. Mo, Y. Tian, B. Wang, H. Zhang, and Z. Zhong, *Phys. Rev. D* **98**, 124025 (2018), arXiv:1808.03635 [gr-qc].
- [46] H. Liu, Z. Tang, K. Destounis, B. Wang, E. Papantonopoulos, and H. Zhang, *JHEP* **03**, 187 (2019), arXiv:1902.01865 [gr-qc].
- [47] S. Hod, *Int. J. Mod. Phys. D* **29**, 2042003 (2020), arXiv:2012.01449 [gr-qc].
- [48] R. H. Price, *Phys. Rev. D* **5**, 2419 (1972).
- [49] P. R. Brady, C. M. Chambers, W. Krivan, and P. Laguna, *Phys. Rev. D* **55**, 7538 (1997), arXiv:gr-qc/9611056.
- [50] P. R. Brady, C. M. Chambers, W. G. Laarakkers, and E. Poisson, *Phys. Rev. D* **60**, 064003 (1999), arXiv:gr-qc/9902010.
- [51] C. Molina, D. Giugno, E. Abdalla, and A. Saa, *Phys. Rev. D* **69**, 104013 (2004), arXiv:gr-qc/0309079.
- [52] R. A. Konoplya and A. Zhidenko, *Phys. Rev. D* **106**, 124004 (2022), arXiv:2209.12058 [gr-qc].
- [53] R. A. Konoplya, *Phys. Rev. D* **109**, 104018 (2024), arXiv:2401.17106 [gr-qc].
- [54] A. Lopez-Ortega, *Gen. Rel. Grav.* **38**, 743 (2006), arXiv:gr-qc/0605022.
- [55] A. Lopez-Ortega, *Gen. Rel. Grav.* **38**, 1565 (2006), arXiv:gr-qc/0605027.
- [56] A. Jansen, *Eur. Phys. J. Plus* **132**, 546 (2017), arXiv:1709.09178 [gr-qc].
- [57] R. A. Konoplya, *Phys. Lett. B* **838**, 137674 (2023), arXiv:2210.08373 [gr-qc].
- [58] H. Kodama and A. Ishibashi, *Prog. Theor. Phys.* **110**, 701 (2003), arXiv:hep-th/0305147.
- [59] A. Ishibashi and H. Kodama, *Prog. Theor. Phys.* **110**, 901 (2003), arXiv:hep-th/0305185.
- [60] H. Kodama and A. Ishibashi, *Prog. Theor. Phys.* **111**, 29 (2004), arXiv:hep-th/0308128.
- [61] Z. Stuchlík and S. Hledík, *Acta Phys. Slov.* **52**, 363 (2002), arXiv:0803.2685 [gr-qc].
- [62] E. W. Leaver, *Proc. Roy. Soc. Lond. A* **402**, 285 (1985).
- [63] C. Gundlach, R. H. Price, and J. Pullin, *Phys. Rev. D* **49**, 883 (1994), arXiv:gr-qc/9307009.
- [64] H.-P. Nollert, *Phys. Rev. D* **47**, 5253 (1993).
- [65] A. Zhidenko, *Phys. Rev. D* **74**, 064017 (2006), arXiv:gr-qc/0607133.
- [66] R. A. Konoplya, D. Ovchinnikov, and B. Ahmedov, *Phys. Rev. D* **108**, 104054 (2023), arXiv:2307.10801 [gr-qc].
- [67] R. A. Konoplya, *Phys. Rev. D* **107**, 064039 (2023), arXiv:2210.14506 [gr-qc].
- [68] A. F. Zinhailo, *Phys. Lett. B* **853**, 138682 (2024), arXiv:2403.06867 [gr-qc].
- [69] S. V. Bolokhov, *Phys. Rev. D* **110**, 024010 (2024), arXiv:2311.05503 [gr-qc].
- [70] S. V. Bolokhov, *Phys. Rev. D* **109**, 064017 (2024).
- [71] R. A. Konoplya and O. S. Stashko, *Phys. Rev. D* **111**, 104055 (2025), arXiv:2408.02578 [gr-qc].
- [72] R. A. Konoplya and O. S. Stashko, *Phys. Rev. D* **111**, 084031 (2025), arXiv:2502.05689 [gr-qc].
- [73] A. Dubinsky, *Phys. Dark Univ.* **46**, 101657 (2024), arXiv:2405.08262 [gr-qc].

- [74] W.-L. Qian, K. Lin, C.-Y. Shao, B. Wang, and R.-H. Yue, *Eur. Phys. J. C* **82**, 931 (2022), arXiv:2203.04477 [gr-qc].
- [75] S. Aneesh, S. Bose, and S. Kar, *Phys. Rev. D* **97**, 124004 (2018), arXiv:1803.10204 [gr-qc].
- [76] R. A. Konoplya, *JCAP* **07**, 001 (2023), arXiv:2305.09187 [gr-qc].
- [77] K. A. Bronnikov, R. A. Konoplya, and T. D. Pappas, *Phys. Rev. D* **103**, 124062 (2021), arXiv:2102.10679 [gr-qc].
- [78] M. Skvortsova, *Fortsch. Phys.* **72**, 2400036 (2024), arXiv:2311.11650 [gr-qc].
- [79] M. Skvortsova, *Fortsch. Phys.* **72**, 2400132 (2024), arXiv:2405.06390 [gr-qc].
- [80] K. A. Bronnikov and R. A. Konoplya, *Phys. Rev. D* **101**, 064004 (2020), arXiv:1912.05315 [gr-qc].
- [81] Z. Malik, *EPL* **147**, 69001 (2024), arXiv:2410.04306 [gr-qc].
- [82] Z. Malik, *Int. J. Theor. Phys.* **63**, 128 (2024), arXiv:2409.09872 [gr-qc].
- [83] Z. Malik, *Int. J. Mod. Phys. A* **40**, 2450132 (2025).
- [84] H.-L. Jia, W.-D. Guo, Q. Tan, and Y.-X. Liu, *Phys. Rev. D* **110**, 064077 (2024), arXiv:2406.03929 [gr-qc].
- [85] E. W. Leaver, *Phys. Rev. D* **41**, 2986 (1990).
- [86] V. Cardoso, A. S. Miranda, E. Berti, H. Witek, and V. T. Zanchin, *Phys. Rev. D* **79**, 064016 (2009), arXiv:0812.1806 [hep-th].
- [87] R. A. Konoplya, A. Spina, and A. Zhidenko, (2025), arXiv:2505.01128 [gr-qc].
- [88] R. A. Konoplya and Z. Stuchlík, *Phys. Lett. B* **771**, 597 (2017), arXiv:1705.05928 [gr-qc].
- [89] R. A. Konoplya and A. F. Zinhailo, *Eur. Phys. J. C* **80**, 1049 (2020), arXiv:2003.01188 [gr-qc].
- [90] B. Toshmatov, Z. Stuchlík, B. Ahmedov, and D. Malafarina, *Phys. Rev. D* **99**, 064043 (2019), arXiv:1903.03778 [gr-qc].
- [91] R. A. Konoplya and A. Zhidenko, *JCAP* **11**, 028 (2022), arXiv:2210.04314 [gr-qc].
- [92] Z. Zhu, S.-J. Zhang, C. E. Pellicer, B. Wang, and E. Abdalla, *Phys. Rev. D* **90**, 044042 (2014), [Addendum: *Phys. Rev. D* **90**, 049904 (2014)], arXiv:1405.4931 [hep-th].
- [93] M. Zhang, J. Jiang, and Z. Zhong, *Phys. Lett. B* **806**, 135523 (2020), arXiv:2005.12722 [gr-qc].
- [94] R. D. B. Fontana, P. A. González, E. Papantonopoulos, and Y. Vásquez, *Phys. Rev. D* **103**, 064005 (2021), arXiv:2011.10620 [gr-qc].
- [95] X.-Y. Nan, J. Tan, and J. Jiang, *Eur. Phys. J. C* **83**, 424 (2023).
- [96] A. Chrysostomou, A. S. Cornell, A. Deandrea, H. Noshad, and S. C. Park, (2023), arXiv:2310.07311 [gr-qc].
- [97] A. Chrysostomou, A. S. Cornell, A. Deandrea, and S. C. Park, (2025), arXiv:2501.14834 [gr-qc].
- [98] P. Liu and R.-D. Zhu, *JHEP* **06**, 015 (2025), arXiv:2412.18359 [hep-th].